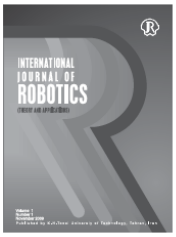

INTERNATIONAL JOURNAL OF ROBOTICS
(THEORY AND APPLICATIONS)
E-mail: IJR@kntu.ac.ir

Road Departure Avoidance System Based on the Driver Decision Estimator

M. Alirezaei[a], A. Ghaffari[a], R. Kazemi[a], M. Corno[b,c], D. Katzourakis[c]

a- Mechanical Engineering Department, K. N. Toosi University, Iran
b- Delft Center for Systems and Control, 3Intelligent Automotive Systems (IAS)
c- Mechanical, Maritime and Materials Engineering (3mE), Technical University of Delft (TUDelft), Delft, Netherlands

ARTICLE INFO

Keywords:
Driving simulation, robust control, road departure avoidance, steer-by-wire, haptic-feedback, shared control.

ABSTRACT

In this paper a robust road departure avoidance system based on a closed-loop driver decision estimator (DDE) is presented. The main idea is that of incorporating the driver intent in the control of the vehicle. The driver decision estimator computes the vehicle look ahead lateral position based on the driver input and uses this position to establish the risk of road departure. To induce a risk of road departure, the proposed system is implemented on a driving simulator and thirty test drivers were asked to avoid a pylon-confined area (obstacle) while keeping the vehicle within the road limits. The RDA systems intervened by applying a haptic-feedback and correcting the steering angle in the event that a vehicle road departure was likely to occur. The experimental results showed that the proposed system reduced workload and effectively helped drivers to stay within road limits.

1-Introduction

Increasing vehicle safety is an important issue as traffic safety reports show that in 2007 about 41000 people were killed and 2.5 million were injured on roads in the USA alone [1]. Most of these car accidents are associated with drivers' errors such as impairment, inattention, fatigue or distraction [2]. Unintended lane departure is one of the most dangerous results of the driver's error. Jermakian [3] estimated the hazardous of lane departure, using crash records files from 2004 to 2008, of the National Automotive Sampling System General Estimates System and the Fatality Analysis Reporting System. Lane departure appears relevant to 179,000 crashes per year and affined to the greatest number of fatal crashes; up to 7,500 fatal crashes per year [3] in the United States. LDW systems have been designed to mainly operate in freeways and arterial roads by helping the driver to stay in the lane of travel. The scope of such systems is to avoid crashes or mitigate crash severity. Since 2001, Nissan motors started offering in Japan a lane keeping support system [4], with an audible feedback, when the vehicle begins crossing the lane markings/limits. Toyota and Honda, in 2002 and 2003, launched their lane keeping assist systems by applying a steering wheel torque to help keeping the vehicle within the lane limits. Nowadays, the majority of the high end automobile manufactures (Mercedes, Volvo, BMW, Nissan-Infiniti, Honda etc.) offer similar assist systems in their top-class models. Most of the LDW systems, utilize a camera to track road markings and to estimate the vehicle position relative to the road. The feedback to the driver varies from audible, visual and/or vibro-tactile signals, up to haptic steering wheel feedback. Nissan (Infiniti) was the first automaker to offer lane departure prevention (LDP), an extension of LDW [5]. The LDP system, in addition to the warning (which is automatically enabled when the vehicle is started), slightly brakes the wheels to help preventing an unintended departure from its travelling lane. Due to the active nature of the system's intervention, Infiniti decided to require drivers to enable the LDP system at will. Infiniti, by considering all of the

factors that are likely to influence the effectiveness of their system, predicts that, if LDP were fitted to all vehicles, some 12% of all road fatalities—around 5,000 deaths—could be prevented annually [6]. Braitman et al. [5] using telephone interviews to Infiniti owners equipped with LDW and LDP, investigated drivers' use and acceptance of these systems. From the interviews conducted for the LDW system, 69% reported that they always drive with the system on, 37% reported that there is nothing they dislike about the system, and 41% reported that the system is annoying. 71% reported that they drift from their lanes less often. Regarding the LDP system, 15% always drive with the system enabled, 50% reported that there is nothing they dislike about it and 23% said the system is annoying. 68% reported that they drift from their lanes less. Interestingly, 22% were unaware they had LDP technology.

In the recent years, extensive researches have focused on designing a shared control between human and road departure avoidance systems. Griffiths and Gillespie [7] explore the benefits of augmented force-feedback (FF) to share control between the driver and automated steering to support lane keeping. Mulder et al. [8] propose a haptic guidance system where both the driver and the support system share the steering wheel control. The authors depict that continuous haptic support is an efficient way to support drivers during curve negotiation. This assertion concurs with continuous haptic steering support system for an obstacle avoidance designed by Penna et al. [9]. The proposed system reduced the number of crashes, the control effort and activity in critical situations. Studies on vibro-tactile feedback for collision mitigation [10] and for learning a lane-keeping task have shown rather promising results [11]. De Winter and Dodou [12] argue that opposed to continuous assist, support during critical manoeuvres is what is important. Sheridan [13] revises several concepts and terms used in human-machine interaction engineering by, distinguishing between the various controls concepts, suggesting "taxonomies for supervisory and direct control" and by defining "human supervisory adaptation". Minoiu [14] developed a switching strategy to involve the driver decision. The proposed system switched on when the hazardous condition is detected and neglects the driver decision. To avoid the need of on/off activation strategy, a model predictive controller is used to plan vehicle future optimal trajectory through the road borders [1]. This predicted trajectory is used to calculate a factor which indicates the hazard level. Based on this factor, the level of controller intervention required to prevent road departure is calculated and controller/driver inputs are scaled accordingly. In case of false activation they heavily modify the behaviour of the vehicle and for this reason are not well accepted [15]. Cerone et al. [16] developed a method which relies on an open loop estimation of the driver intention. This may introduce a control action also when not needed.

Triggered by the aforementioned fruitful results, a robust road departure avoidance (RDA) system was developed. This RDA system utilizes look-ahead information to derive the future lateral position of the vehicle with respect to the road. The proposed system intervenes by applying a feedback-torque and correcting the front wheels' angle in the event that a road departure is likely to occur. The controller is based on a closed-loop system that incorporates the driver's intentions; likewise [7], [8], [16]. To assess the performance of the proposed system, it is implemented on a driving simulator and thirty test drivers executed a driving task with supported and unsupported setup. They were instructed to avoid an obstacle while keeping the vehicle within the road limits.

The content of the paper is organized as follows. In Section 2, the vehicle model is described. The structure of the proposed method is given in Section 3 and the concept of the DDE is introduced. In Section 4 the robust controller is designed. In Section 5 the experimental studies are described, where the test manoeuvre and participants are introduced. The results are analysed in Section 6 and finally conclusions are drawn in Section 7.

2- Vehicle Dynamic

For the design of the vehicle lateral control, a fourth order linear model has been used (Fig. 1) [15], i.e.,

$$\begin{aligned} \dot{x} &= Ax + Bu + E\rho \\ y &= Cx \end{aligned} \tag{1}$$

The state vector $x = (v, r, y_{la}, \psi_{vr})^T$ contains the following components, the vehicle lateral velocity (v), the yaw rate (r), the lateral offset of the C.G. from the centreline, taken at a look ahead distance (y_{la}) and the relative yaw angle (ψ_{vr}). δ is the steering angle of the front wheels, ρ is the road curvature. A, B, C and E are given,

$$A=\begin{bmatrix} a_{11} & a_{12} & 0 & 0 \\ a_{21} & a_{22} & 0 & 0 \\ 1 & x_{la} & 0 & u \\ 0 & 1 & 0 & 0 \end{bmatrix}, B=\begin{Bmatrix} C_f/m \\ aC_f/I_z \\ 0 \\ 0 \end{Bmatrix}, E=\begin{Bmatrix} 0 \\ 0 \\ 0 \\ -u \end{Bmatrix}, C=\begin{Bmatrix} 0 & 0 & 1 & 0 \end{Bmatrix},$$

$$a_{11}=-(C_r+C_f)/mu, \qquad a_{12}=(bC_r-aC_f)/mu-u,$$

$$a_{21}=(bC_r-aC_f)/I_z u, \qquad a_{22}=-(b^2C_r+a^2C_f)/I_z u.$$

From (1), the transfer function matrix from the steering angle to y_{la} is:

$$G(s)=\frac{y_{la}(s)}{\delta(s)}=C(sI-A)^{-1}B=\frac{m_2 s^2+m_1 s+m_0}{s^2(n_2 s^2+n_1 s+n_0)} \tag{2}$$

The integrators arise from positional states and two other poles determine the vehicle handling.

Note that the model, although simple, is suitable for highway traffic. In fact unmodelled dynamics are little excited in highway driving, usually characterized by slow steering action, slow velocity variation and small pitch and roll angles. The nominal parameters used in the model are shown in Table 2.

The remaining symbols are:

x_{la}	look ahead distance
m	vehicle mass
u	longitudinal velocity
I_z	vehicle yaw moment of inertia
C_f	cornering stiffness of front tires
C_r	cornering stiffness of rear tires
a	distance from C.G. to front axle
b	distance from C.G. to rear axle

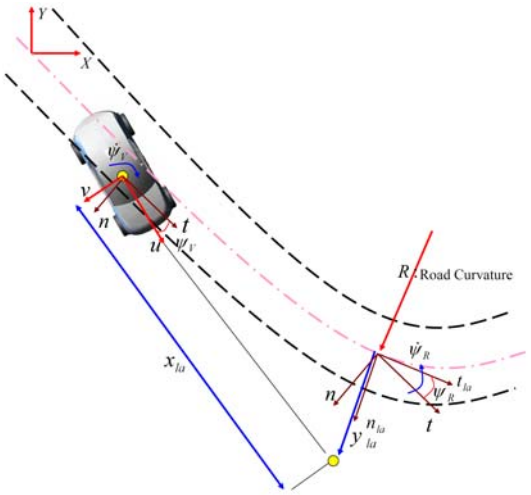

Fig. 1: Vehicle and road reference frames.

3- Framework Description

In this section, the novel road departure avoidance system which works based on the driver decision estimator (DDE) will be presented. The important outcome of using DDE is accounting for driver intent which is critical for the user acceptance of the driver assistant systems (DAS).

3-1- Control structure

The structure of the proposed system is shown as a block diagram in Fig. 2. Block G represents the vehicle dynamics from the front wheels' angle δ to y_{la}; $\hat{G}$ is the estimate of G. $\hat{G}$ has been used to accommodate for the modeling error and the parameter uncertainty of G. The saturation is used to define the safe region for y_{la} as shown in Fig.3. As can be seen in the block diagram, y_{la} is computed as,

$$y_{la} = G\delta = G\left(\delta_C + \delta_d\right) \tag{3}$$

where δ_c is the G_c H_∞ controller's correcting angle and δ_d the wheels angle from the driver's steering wheel angle θ_{sw}.

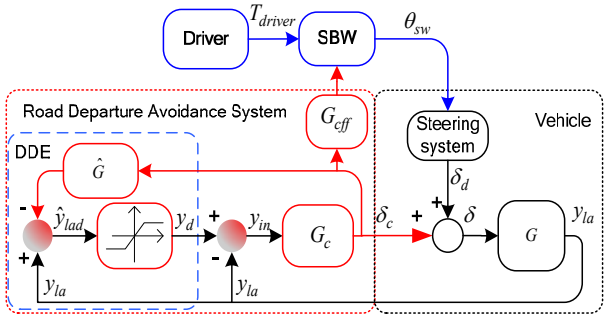

Fig. 2: Block diagram of the proposed method.

The driver desired lateral offset (y_{lad}) between the vehicle C.G. and the centerline at the look ahead distance is defined as,

$$y_{lad} = G\delta_d \,. \tag{4}$$

According to (3) and (4) y_{lad} is calculated as,

$$y_{lad} = y_{la} - G\delta_C \,. \tag{5}$$

The control signal (δ_C), is computed as,

$$\delta_C = G_C\left(y_d - y_{la}\right) \tag{6}$$

where, y_d is the desired lateral offset accounting for driver's demand and road limitation, which is defined,

$$y_d = \eta\hat{y}_{lad} + \lambda\,, \tag{7}$$

$\hat{y}_{lad}$ is the estimation of the driver desired lateral offset between the vehicle C.G. and centreline taken at the look ahead distance. It is computed in the proposed DDE as,

$$\hat{y}_{lad} = y_{la} - \hat{G}\delta_C \tag{8}$$

Also η and λ are the parameters for describing the saturation nonlinearity as a mathematical function,

$$\begin{aligned} &if\left(\hat{y}_{lad} < -y_L\right) \Rightarrow \eta = 0 \quad and \quad \lambda = -y_L \\ &if\left(\left|\hat{y}_{lad}\right| \le y_L\right) \Rightarrow \eta = 1 \quad and \quad \lambda = 0 \\ &if\left(\hat{y}_{lad} > y_L\right) \Rightarrow \eta = 0 \quad and \quad \lambda = y_L \end{aligned} \tag{9}$$

where y_L is the lane border.

Substituting (6)-(9) into (3), y_{la} can be written as a function of δ_d, η and λ,

$$y_{la} = \frac{(1+\eta G_C\hat{G})G}{1+G_CG+\eta G_C(\hat{G}-G)}\delta_d + \frac{G_CG}{1+G_CG+\eta G_C(\hat{G}-G)}\lambda \tag{10}$$

Depending on the status of the saturation the following cases are given:

$$\begin{aligned} &if\left(\hat{y}_{lad} < -y_L\right) \Rightarrow y_{la} = \frac{G}{1+GG_C}\delta_d - \frac{GG_C}{1+GG_C}y_L \\ &if\left(\left|\hat{y}_{lad}\right| \le y_L\right) \Rightarrow y_{la} = y_{lad} \\ &if\left(\hat{y}_{lad} > y_L\right) \Rightarrow y_{la} = \frac{G}{1+GG_C}\delta_d + \frac{GG_C}{1+GG_C}y_L \cdot \end{aligned} \quad (11)$$

According to equation (11), when the estimation of driver desired lateral offset is in the safe region, the controller has no effect on the system. When the saturation is activated, implying that the vehicle is pointing toward an unsafe area. The driver demand is considered as a disturbance for the control system.

3-2- Steering setup

The RDA setup combines an "input-mixing shared control" with a "haptic shared control" as defined by Abbink and Mulder [17] influencing both steering angle as well as the FF on the control interface. The rationale of these setups is that when the driver cannot overrun an assist system, he/she should at least be aware of the system's activity by force information. Switkes et al. [18] studied a steer-by-wire (SBW) system generating the correct steering input to ensure good lane-keeping performance while at the same time the FF driving from a potential field, acts towards the direction which minimizes the potential.

The SBW approach allows decoupling the steering wheel from the wheels thus giving an extra degree of freedom to assist the driver. The SBW follows the "input-mixing shared control" [17]. It applies a corrective steering angle δ_c (c.f. Fig. 2) to prevent road departure by altering the relation between the driver's input δ_d and final wheels angle δ. Also the haptic-feedback (HF) applies a guiding HF assisting the driver to avoid road departure. The haptic-force is the product of correcting angle δ_c and a stiffness term.

Equation (12) is a simplified illustration of how the steering FF is calculated. It consists of multiple terms, which are activated according to the RDA setup. The $VTires_{ff}$ (virtual-tires FF) represents the FF applied on the steering wheel resulting from the front left/right tire lateral forces (f_{fly}, f_{fry}), as a function of the driver's wheels angle δ_d. The virtual tires are only used for determining the steering FF; the tires from the simulator are used in the vehicle simulation for determining the tire forces at the wheel. The virtual tire forces are calculated as a function of the tire slip using the Pacjeka's Magic Formula [19]. Tire slips refer to the non-dimensional relative velocity of the tire with respect to the road and are calculated as in (13).

$$J\ddot{\theta}_{sw} = T_{driver} - VTires_{ff} + G_{cff} + T_{assist}(T_{driver})$$

$$VTires_{ff} = (f_{fly} + f_{fry}) \cdot G_{F2T} \quad (12)$$

$$G_{cff} = K_c \cdot \delta_c$$

$$s_{fjy} = (1 + s_{fjx})\hat{V}_{fjy} / \hat{V}_{fjx} \quad (13)$$

$$\hat{V}_{fjx}, \hat{V}_{fjy} : Q(u, v, r, \delta_d, a, t_r) \quad (14)$$

$$f_{jly} = \mu(s_{fjy}, s_{fjx}) \cdot F_{fjz}, \quad j : l, r \quad (15)$$

The tires' velocities are a function Q of the vehicle's speed *u, v, r* (yaw rate) and the suspension geometry properties (*a, t_r*). When $\delta c \neq 0$ (c.f. Fig. 2) it will result to a change to the vehicle's states (*u, v, r*) which will develop a lateral slip s_{fjy}, creating a guiding HF towards to direction that the RDA controller is steering. This justifies the use of hat (^) in (13) and (14). The longitudinal slip s_{fjx} used in (13), and the normal forces F_{fjz} in (15) originate from the simulator. The final lateral forces are a function μ of the s_{fjx} and s_{fjy}. Table 1 summarizes the parameters and variables within (12)-(15).

The G_{cff}, is a HF term, product of correcting angle δ_c (resulting from the G_c) and a stiffness term K_c. It serves as a guiding torque towards the direction that the G_c wants to steer the vehicle. The T_{assist} constitutes a power assist force designed as driver torque-depended lookup table found in modern vehicles [20]. The solution of equation (12) will dictate the steering wheel velocity $d\theta_{sw}/dt$, which constitutes the command being sent to the velocity-controlled FF motor [21].

Table. 1: RDA steering setups' parameters and variables.

Name	Description	Name	Description
J	Steering system moment of inertia (kg·m2)	T_{driver}	Driver's torque (Nm)
G_{F2T}	Front wheels' lateral wheel forces to steering torque gain	T_{assist}	Assist torque (Nm)
s_{fjy}	Front left/right (j: l, r) tires y lateral slip	s_{fjx}	Front left/right (j: l, r) tires y longitudinal slip
F_{fjz}	Front left/right (j: l, r) tires normal load	t_r	Vehicle trackwidth (m)
K_c	RDA stiffness (Nm/rad)	$\hat{V}_{fjx}, \hat{V}_{fjy}$	Front left/right (j: l, r) tires x, y velocity

4- Robust Controller Design

In this section a robust road departure avoidance system is designed. The controller is designed based on a reduced order vehicle-road model and considering both dynamic and parametric uncertainties. The choice of the reduced order model yields a low order controller that is tunable.

4-1-Model reduction

The model derived in Section 2 can be reduced using the balanced truncation method [22]. The state space of the reduced order model is determined as,

$$\hat{A}=\begin{bmatrix}0 & u\\ 0 & 0\end{bmatrix},\hat{B}=\begin{Bmatrix}\left(\frac{(x_{la}+b)}{u}-\frac{m_r u}{C_r}\right)\\ \frac{1}{u}\end{Bmatrix}f_0,\hat{E}=\begin{Bmatrix}0\\ -u\end{Bmatrix},\hat{C}=\begin{bmatrix}1 & 0\end{bmatrix},$$

where, $l=a+b$, $m_r=ma/l$ and $f_0=1/(l/u^2+K_{us})$. According to the vehicle nominal parameters (Table 2), $m_r u/C_r$ is negligible compared to $(x_{la}+b)/u$. Also x_{la} □ b so the input coefficient matrix ($\hat{B}$) is,

$\hat{B}=\{x_{la}f_0/u \quad f_0/u\}$.

The transfer function of the reduced order model is then,

$$\hat{G}(s)=\frac{f_1 s+f_0}{s^2} \qquad (16)$$

where, $f_1=x_{la}f_0/u$. Fig. 3 represents the bode diagram of the original vehicle model and the reduced order model. As it can be seen, the reduced order model provides a good approximation up to 10 rad/s.

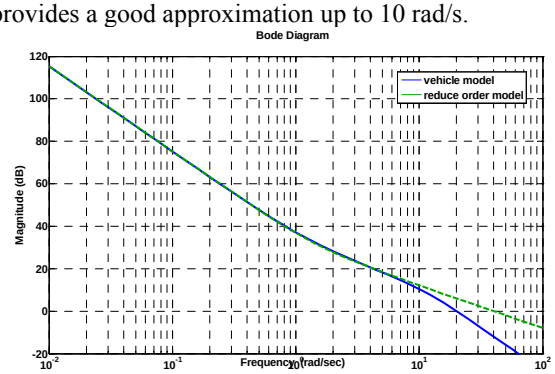

Fig. 3: Comparison of the bode diagrams of the original model and the reduces one

4-2-Model uncertainty

The reduced order model is affected by two sources of error: the order reduction and parameters uncertainty. These modelling errors are modelled as multiplicative uncertainty [23]:

$$G(s)=(1+W_m(s)\Delta_m(s))\hat{G}(s),\quad |\Delta_m(j\omega)|\le 1,\quad \forall\omega \qquad (17)$$

where $\hat{G}(s)$ is the transfer function of the nominal reduced order plant, $\Delta_m(s)$ is a normalized complex function which represents parametric and dynamic modeling errors, and $W_m(s)$ is a known conservative function bounding the modeling error.

A description of $\Delta_m(s)$ based on vehicle complex uncertainty is illustrated in Fig. 4. The conservative bound on modelling error is derived as,

$$W_m(s)=\left(\frac{s+.5}{s+1}\right)^2. \qquad (18)$$

The mentioned weighting functions are used to model dynamic uncertainties and parametric uncertainties such as mass and tires cornering stiffness which are varying and are difficult to measure.

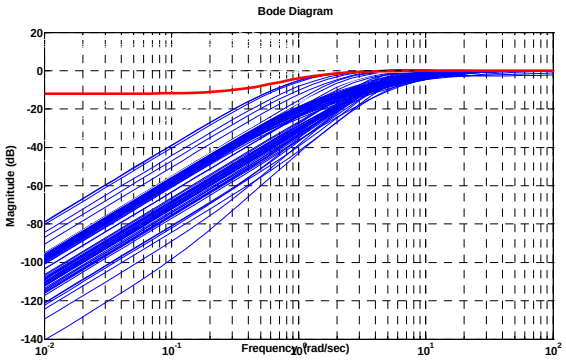

Fig. 4: Complex uncertainty of vehicle $\Delta_m(s)$ and weighting function $W_m(s)$ (Solid line)

Table. 2: Vehicle parameters with uncertainty

Parameter	Uncertainty Value	Nominal Value
m	1100-1500 Kg	1278 Kg
C_f	46680-93360 N/rad	93360 N/rad
C_r	28670-57340 N/rad	57340 N/rad
a	-	0.9 m
b	-	1.7 m
u	30– 100 km/h	50 km/h
x_{la}	-	10 m

4-3-H_∞ controller

According to (11) the DDE and the estimated model only determine the activation of the road departure avoidance system. When it is active the saturation block generates a reference that the controller tracks. Thanks to these considerations the closed loop controller can be designed neglecting the DDE and focusing only on the vehicle dynamics.

To guarantee robustness an H_∞ controller is designed based on the interconnection scheme shown in Fig. 5. The reference model design approach is easily recognized from the scheme.

The design relies on the definition of several weighting functions:

- $G_{ref}=1/(0.23s+1)$ represents the reference model. It defines the desired response of the vehicle. According to the nominal vehicle speed and look ahead distance, when the lateral offset at the look ahead distance is toward an unsafe area it takes 0.7 seconds for the vehicle to reach the unsafe area. Based on that the bandwidth has been chosen to guarantee that in the nominal condition the system has enough time to intervene before reaching the road limits.
- The model matching error in the lateral displacement channel is weighted by $W_s(s)=0.1(s+1)/(s+0.001)$. It penalizes the low frequency matching error, guaranteeing a small DC-error.
- The weighting filter $W_u(s)=10\times(s+1)/(s+10)$ captures the limit on the steering system. This

choice penalizes the magnitude and rate of the actuator.

- According to the proposed block diagram (Fig. 5) and the active steering system architecture, the driver's steering action is considered as disturbance for the control system. So, W_d is used to capture the disturbance acting on the plant. In this scheme the driver's steering input can be modelled as a low pass filter [18].
  $W_d(s) = 0.1\times(s+10)/(s+1)$.
- High pass filters $W_n(s) = 0.01\times(s+1)/(s+100)$ are used to model the frequency content of the sensors noise in the lateral displacement and the yaw rate channels.

Using standard techniques it is possible to design a robust controller G_c that satisfies the robust stability condition.

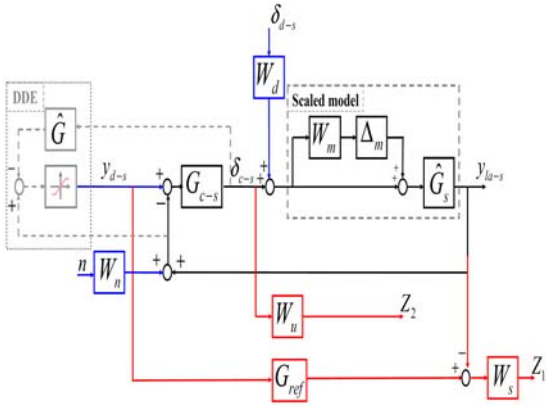

Fig. 5: The block diagram in terms of scaled variables.

4-4-Robust stability

To analyze the robust stability of the system in Fig. 5, we rearrange it into an $M\Delta-structure$, where M is the transfer function from input to output of the perturbation which is calculated as [23],

$$M = -W_m G_C G(1+G_C G)^{-1} \tag{19}$$

For a system with complex unstructured uncertainty, the $M\Delta-structure$ is robust stable for perturbation Δ satisfying $\|\Delta\|_\infty \le 1$, if and only if $\bar{\sigma}(M(j\omega)) < 1 \quad \forall\omega$ or $20\log(\bar{\sigma}(M(j\omega))) < 0 \quad \forall\omega$. Where $\bar{\sigma}$ is the singular value. The singular value of M for different frequency is shown in Fig. 6. As it can be seen the control system is robustly stable.

5-Experimental Studies

The driver-in-the-loop testing of the RDA controller was conducted on the X-Car moving base simulator of the *Intelligent Automotive Systems* (IAS) group; see Fig. 7. The simulator is based on a dSPACE

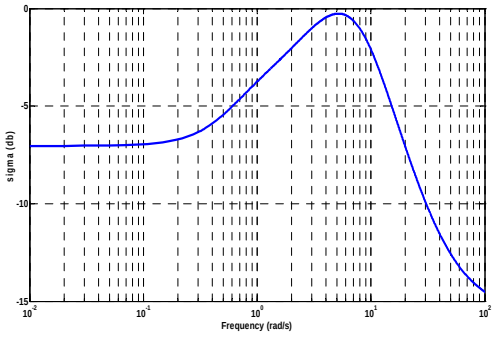

Fig. 6: Singular values of *M*

real-time (RT) computer and runs a commercial RT vehicle dynamics model (VDM), developed on an open Matlab®/Simulink® block, from the dSPACE Automotive Simulation Model (ASM) package. The vehicle is an open Matlab®/ Simulink® model with 24 DOF. It incorporates semi-empirical tire models, suspension dynamics, and steering system model.
The VDM model is being executed at 1 kHz (1 ms fixed time step); the communication with the environment through interface boards and the motion-responsible controllers are executed at 5 kHz. A detailed description can be found in [21]. The ASM VDM from dSPACE has provisions to calculate the future position of the vehicle and correspondingly the lateral offset with respect to the road. The RDA system (c.f. Fig. 2) was therefore fed with the y_{la} signal deriving from the ASM VDM. The look-ahead time, determining the length of x_{la} (c.f. Fig. 1).

Fig. 7: The X-Car TUDelft driving simulator.

5.1 Test manoeuvres

To induce the risk of a road departure, during an evasive-manoeuvre, the test drivers were asked to avoid a pylon-confined area (obstacle) while keeping the vehicle within the road limits Y = [-3: 3] m.
The driving task is pictured in Fig.8. The front wheel drive vehicle started with 0 km/h and automatically

accelerated up to a fixed speed of 50 km/h (reached around X = 30 m). The tests drivers were instructed to drive straight in the centre of the road (6 m in width; Y = [-3:3] m) and steer at end of the pylon-confined passage from X = [70:100] m. They should later pass through the 2.5 m-wide pylon passage from X = [110:130] m, avoid departing and hitting the pylons, and then return to the centre of the road and drive up to the end of the finish line, 205 m away from the Start (c.f. Fig. 2). The RDA system assists the driver to stay within the road width limits, but does not assist to avoid the pylons.

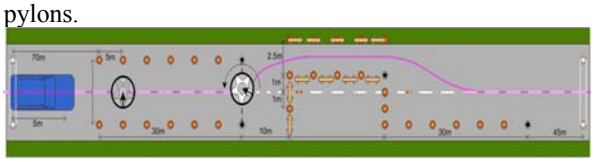

Fig. 8: driving task

5-1- Test participants

Out of the 30 test drivers, 2 were female and all but one had a driver's license. The mean age was 29.7 years (SD = 5.0), their average driven km per year was 10,095 (SD = 10,980), and the average driving license possession was 9.0 years (SD = 6.2). All drivers graded their own driving competence, resulting in a mean score of 6.93 (SD = 1.08) on a scale from 1 to 10, with 1 being an incompetent driver and 10 being an expert.

All test drivers drove the two different setups, the unsupported and supported. The first 20 drivers practiced each unsupported setup for 10 runs and supported setup for 8 runs and their performance was recorded in 3 additional runs. The next 10 drivers practiced unsupported and supported setup for 6 and 8 runs, respectively; and their performance was recorded in additional 7 runs.

After completing each driving setup session, the participant stepped out of the simulator to fill in the NASA Task Load Index (TLX). This questionnaires measures workload on six dimensions (mental demand, physical demand, temporal demand, performance, effort, and frustration level), and has been used in shared control car driving experiments before [24], [25].

6. Results

Fig. 9 shows the average path for the supported and unsupported vehicle. The average path of participants driving without the RDA was smooth and symmetric. Participants driving with the RDA, on the other hand, drove more to the right between X = 110 and 130 m, and appeared to counter-steer [21] around X = 125 m. Furthermore, participants driving with the RDA were slower to get back to lane centre (see X > 140 m).

Fig. 10 shows the average steering wheel angle per setup. Without the RDA, the participants adopted a classical double pulse in order to avoid the obstacle. With the RDA the drivers steered less to the right, (compared to the unsupported) between 110 < X < 120, while they appear to make a second steering pulse to the left (around X = 125 m) to avoid hitting the pylons positioned at Y = 1 m. This was related to the fact that the RDA system would steer the front wheels to prevent a road departure faster than the drivers, minimizing the need for right steering (starting around X = 100 m). The majority of the drivers did not perceive this and would overshoot the system, driving the cars towards to the pylons (at Y = 1 m) necessitating the observed on-coming counter-steering input around X = 125 m. Furthermore, it can be seen that the steering angle for the supported and unsupported vehicle are similar in X < 110 and X>150. It means the controller intervenes only when the vehicle was about to depart the road; see equation (11).

Fig. 11 shows the average measured drivers' torque. The second steering pulse can again be seen for the supported vehicle (around 115 m).

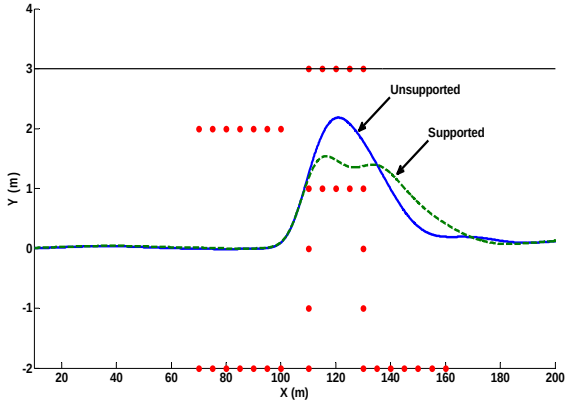

Fig. 9: The average paths of the centre of the vehicle for the supported and unsupported vehicle. The values represent point-wise averages. These averages were calculated first per individual participant and then over all 30 participants. The filled circles represent the positions of the pylons. The horizontal line at Y = 3 m represents the road boundary.

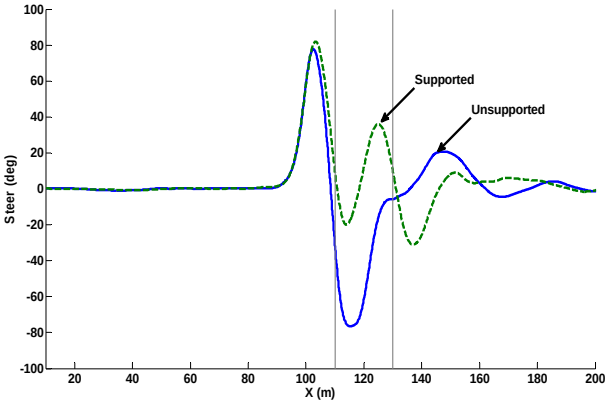

Fig. 10: The average steering wheel angle θ_{sw} for the supported and unsupported vehicle (positive = to the left). The values represent point-wise averages. These averages were calculated first per individual participant and then over all 30 participants. The vertical lines (X = 110 m and X = 130 m) mark the first and last pylon that had to be avoided.

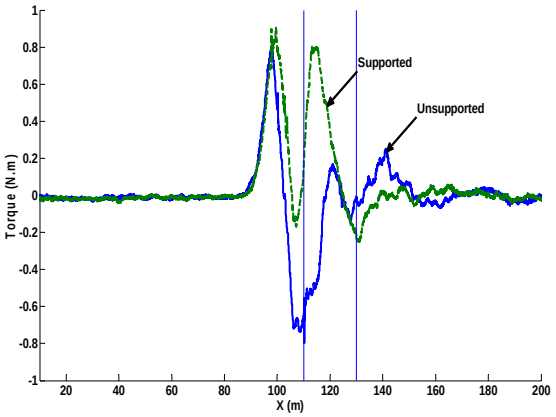

Fig. 11: The average drivers' torque T_{driver} the supported and unsupported vehicle (positive = to the left). The values represent point-wise averages. These averages were calculated first per individual participant and then over all 30 participants. The vertical lines (X = 110 m and X = 130 m) mark the first and last pylon that had to be avoided.

Fig. 12 and Fig. 13 show all the driven paths for the unsupported and supported, respectively. It can be seen that the supported setup prevented road departures. However, the RDA also introduced countersteering behaviour. These results are confirmed in Fig. 14, Fig. 15 showing the steering angle for unsupported and supported vehicle, respectively.

Fig. 16 shows the results of the NASA TLX for measuring workload, revealing small differences only. The supported system resulted in less temporal demand and less effort than unsupported setup. Also the supported system enhanced the performance of the system. The results are confirmed by the objective performance which indicates the RDA system reduced the number of road side departures (Fig. 12 , Fig. 13).

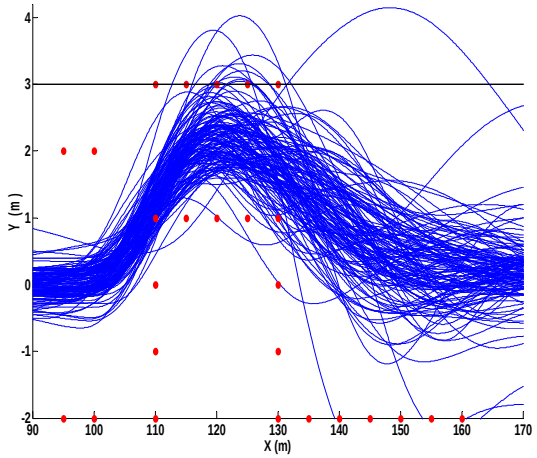

Fig. 12: The paths of the centre of the vehicle for all driven manoeuvres of the unsupported vehicle. The filled circles represent the positions of the pylons. The horizontal line at Y = 3 m represents the road boundary.

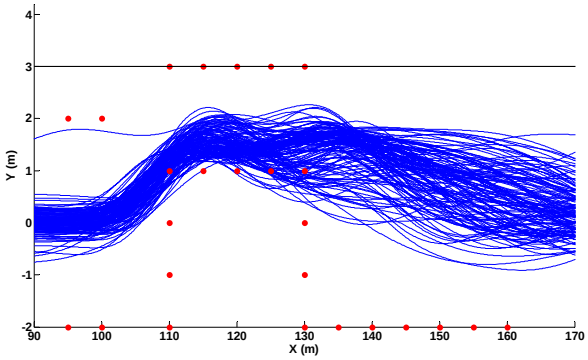

Fig. 13: The paths of the centre of the vehicle for all driven manoeuvres of the supported vehicle. The filled circles represent the positions of the pylons. The horizontal line at Y = 3 m represents the road boundary.

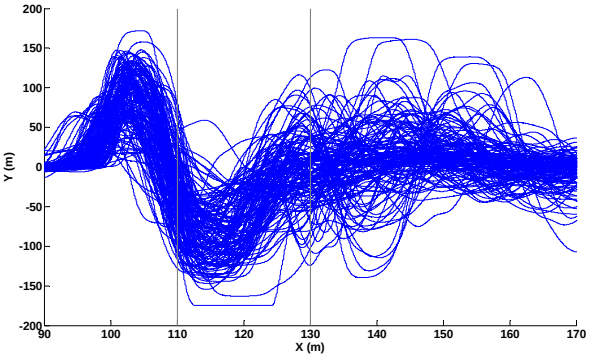

Fig.14: The steering wheel angle θ_{sw} for all driven manoeuvres of the unsupported vehicle. The vertical lines (X = 110 m and X = 130 m) mark the first and last pylon that had to be avoided.

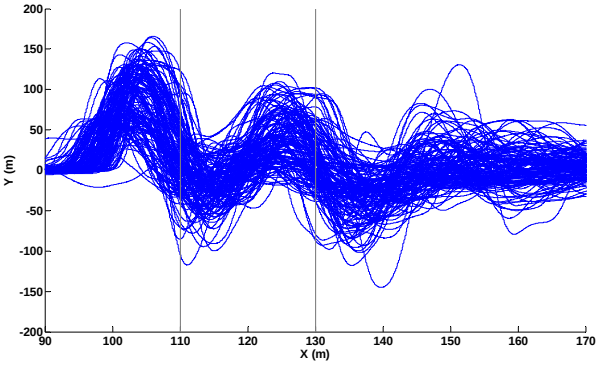

Fig. 15: The steering wheel angle θ_{sw} for all driven manoeuvres of the supported vehicle. The vertical lines (X = 110 m and X = 130 m) mark the first and last pylon that had to be avoided.

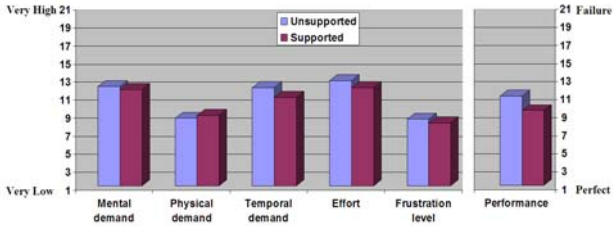

Fig. 16: Means of the NASA Task Load Index.

7. Conclusion

The problem of designing a robust road departure avoidance system has been presented. The proposed approach is based on a closed-loop estimation of the driver intentions. The proposed RDA system has been tested in experiments and has proven capable of avoiding road departures while sharing control with a human driver. The RDA, "input-mixing shared control", reduced workload and effectively helped drivers to keep a safe distance from the detected roadside and promote performance when a road departure is likely to occur. The percentage of road departures (first calculated per participant and then averaged over all 30 participants) were, the unsupported with 52.9%, and Supported 0%. Also it has been shown that the using DDE provided significant autonomy to a human driver and the controller intervening only as necessary to keep the vehicle under safe area.

References

[1] S. J. Anderson and S. C. Peters, An Optimal-control-based Framework for Trajectory Planning, Threat Assessment, and Semi-autonomous Control of Passenger Vehicles in Hazard Avoidance Scenarios, *Int.J. Vehicle Autonomous Systems*, Vol. 8, Ns.2/3/4, 2010.

[2] S. Y. Kim and J.K. Kang (2008), An Intelligent and Integrated Driver Assistance System for Increased Safety and Convenience based on all-around Sensing, *Journal of Intelligent Robot System*, Vol. 51, 261–287.

[3] J. S. Jermakian, "Crash Avoidance Potential of Four Passenger Vehicle Technologies," *Accident Analysis & Prevention*, vol. 43, no. 3, pp. 32-40, Nov. 2010.

[4] C. Schweinsberg, "Infiniti Lane Departure Prevention to Debut on New M." Available: http://wardsauto.com/ar/infiniti_lane_prevention/ Accessed, March 2011.

[5] K. A. Braitman, A. T. McCartt, D. S. Zuby, J. Singer, "Volvo and Infiniti Drivers' Experiences With Select Crash Avoidance Technologies," *Traffic Injury Prevention*, vol. 11, no. 3, pp. 270-278, 2010.

[6] EuroNCAP, Infiniti Departure Prevention System: Available: http://www.euroncap.com/rewards/infiniti_ldp.aspx Accessed, March 2011.

[7] P. Griffiths, R. B. Gillespie, "Sharing Control Between Human and Automation Using Haptic Interface: Primary and Secondary Task Performance Benefits," *Human Factors*, vol. 47, no. 3, pp. 574-590, Fall 2005.

[8] M. Mulder, D. A. Abbink, E. R. Boer, "The effect of haptic guidance on curve negotiation behaviour of young, experienced drivers," in the *2008 Proc. of the IEEE Int. Conf. SMC*, pp. 804–809, Oct. 2008.

[9] M. Della Penna, M. M. van Paasen, D. A. Abbink, M. Mulder, and M. Mulder, "Reducing steering wheel stiffness is beneficial in supporting evasive maneuvers," in the *2010 Proc.* of the *IEEE Int. Conf. Systems, Man and Cybernetics,* Istanbul, Turkey, pp. 1628–1635, 2010.

[10] J. M. Chun, G. Park, S. Oh, J. Seo, S. H. Han, and S. Choi, "Evaluating the Effectiveness of Haptic Feedback on a Steering Wheel for Forward Collision and Blind Spot Warnings," in the *Proc. of the 9th Pan-Pacific Conf. on Ergonomics* (PPCOE), Kaohsiung, Taiwan, 2010.

[11] S. de Groot, J. C. F. de Winter, J. M. L. García, M. Mulder, P. A. Wieringa, "The Effect of Concurrent Bandwidth Feedback on Learning the Lane-Keeping Task in a Driving Simulator," *Human Factors*, vol. 53, no. 1, pp. 50–62, Feb. 2011.

[12] J. C. F. de Winter, D. Dodou, "Preparing drivers for dangerous situations: A critical reflection of continuous shared control," submitted to the *2011 IEEE International Conference on Systems, Man, and Cybernetics* (IEEE SMC 2011), March 2011.

[13] T. B. Sheridan, "Adaptive Automation, Level of Automation, Allocation Authority, Supervisory Control, and Adaptive Control: Distinctions and Modes of Adaptation," *IEEE Trans. on SMC, Part A*, in press, 2011.

[14] N. Minoiu, M. Netto, S. Mammar and B. Lusetti (2009), Driver Steering Assistance for Lane Departure Avoidance, *Control Engineering Practice*, Vol. 17, pp. 642-651.

[15] M. Alirezaei, M. Corno, A. Ghaffari, R. Kazemi, "Robust Road Departure Avoidance Based on Driver Decision Estimation," to be presented in the *2011 IFAC World Congress*, 2011.

[16] V. Cerone, M. Milanese and D. Regruto, "Combined Automatic Lane-Keeping and Driver's Steering Through a 2-DOF Control Strategy," *IEEE Transactions on Control Systems Technology*, vol. 17, no.1, pp. 135-142, Jan. 2009.

[17] D. A. Abbink, M. Mulder, *Advances in Haptics*, InTech, pp. 499-516, April 2010.

[18] J.P. Switkes, Handwheel Force Feedback With Lanekeeping Assistance: Combined Dynamics, Stability and Bounding, a dissertation of doctor of philosophy, Stanford University, 2005.

[19] E. Bakker, L. Nyborg, H. Pacejka, "Tyre modelling for use in vehicle dynamics studies," SAE Paper No. 870421, 1987.

[20] Volkswagen AG, Wolfsburg, Service Training, Self-study programme 317, "The electro-mechanical power steering with dual pinion, Design and function." Available:

http://tos.pp.fi/koukku/892403.pdf Accesed, March 2011.

[21] D. Katzourakis, D. Abbink, R. Happee, E. Holweg, "Steering Force-Feedback for Human Machine Interface Automotive Experiments," *IEEE Transactions on Instrumentation and Measurement*, vol. 60, no. 1, 2011, Special Issue on Haptic Enabled Virtual Environments.

[22] U. Mackenroth, Robust Control Systems Theory and Case Study, chapter 9, Springer, Germany, 2004.

[23] S. Skogestad, and I. Postlethwaite, Multivariable Feedback Control, chapter 1, 7, 9, 10, 11, 2nd edition, John Wiley, England, 2007.

[24] S. G. Hart, L. E. Staveland, "Development of NASA-TLX (task load index): Results of empirical and theoretical research," in *Human Mental Workload*, P. A. Hancock and N. Meshkati, Eds. Amsterdam, The Netherlands: North Holland, pp. 139–183, 1988.

[25] J. C. F. de Winter, M. Mulder, M. M. van Paassen, D. A. Abbink, P. A. Wieringa, "A two-dimensional weigh function for a driver assistance system," *IEEE T. Syst. Man Cyb. B*, vol. 38, no. 1, pp. 189–195, Feb. 2008..